Available online at www.sciencedirect.com
SCIENCE DIRECT
Journal of Power Sources 154 (2006) 428–436
JOURNAL OF POWER SOURCES
www.elsevier.com/locate/jpowsour

Efficiency enhancement in gasoline reforming through the recirculation of reformate

J. Schäfer [a,*], M. Sommer [b], S. Diezinger [c], D. Trimis [c], F. Durst [c]

[a] *DaimlerChrysler AG, RBP/AS, 89081 Ulm, Germany*
[b] *DaimlerChrysler AG, RTC/A, 70567 Stuttgart, Germany*
[c] *FAU Erlangen-Nurnberg, LSTM, 91031 Erlangen, Germany*

Abstract

Fuel processors for on-board hydrogen production have to meet numerous technical demands. They should be efficient, compact and lightweight, capable of different loads and able to perform cold start ups. In this paper, the recirculation of reformate is proposed as a means of efficiency enhancement. Different system configurations based on this idea are introduced and simulated. The resulting effect on the system's efficiency, the water balance as well as the impact of recirculation on the system's volume and weight are discussed.

Keywords: Gasoline reforming; Efficiency; System configuration; Recirculation

1. Introduction

Many techniques that are essential to high-class car convenience, such as air conditioners, mobile office and multi media applications, increase the demand of electrical energy. Therefore, the sufficient supply of this energy is a key to customer's comfort in premium automobiles.

The need to satisfy this increasing demand of electrical energy on the one hand, and the goal to reduce the consumption of energy and emissions on the other hand, stress the necessity to develop efficient means of on-board energy supply. In this context, auxiliary power units (APUs) based on fuel cells are an interesting option, since fuel cell systems have the potential to be low emission, efficient and of high power density.

Systems comprised of different types of fuel cells and fuel processors have been proposed for this application [10,8,6,1]. With respect to their potential in terms of efficiency, systems connecting solid oxide fuel cells (SOFCs) with partial oxidation (POx). Reformers and polymer electrolyte fuel cells (PEMFCs) with steam reformers (SR) seem to be the most promising combinations. Due to the general capability of PEMFCs to stand thermo cycles, perform fast cold start ups and handle different loads, systems based on this type of fuel cell seem to be the more promising option at the current stage of development.

This paper focuses on a fuel cell system based on hydrogen-driven PEMFC, a steam reformer and a hydrogen selective membrane. The system setup and its assessment criteria are introduced in Sections 2 and 3, respectively. Section 4 gives a short description of the model that is used to evaluate different systems. In Section 5, the recirculation of reformate is suggested based on an analysis of the influence of the steam to carbon ratio and a review of the system configuration. Several potential system configurations are presented. In Section 6, the effects of the proposed method are simulated using Aspen Plus. Results are presented for different system configurations, operational modes and parameter sets followed by a comparison with respect to the introduced assessment criteria. Moreover, a selected system is analyzed in detail showing the effect of recirculation on hydrogen concentration and yield. Furthermore, the impact on the water balance as well as on system's efficiency, volume and weight is discussed. Finally, the results are summarised and future activities are outlined.

2. The system setup

The fuel processing and fuel cell system under examination consists of a PEM fuel cell (FC), a steam reformer (SR) and a

* Corresponding author. Fax: +49 711 3052141069.
E-mail address: Jochen.Schaefer@DaimlerChrysler.com (J. Schäfer).

0378-7753/$ – see front matter © 2006 Published by Elsevier B.V.
doi:10.1016/j.jpowsour.2005.10.028

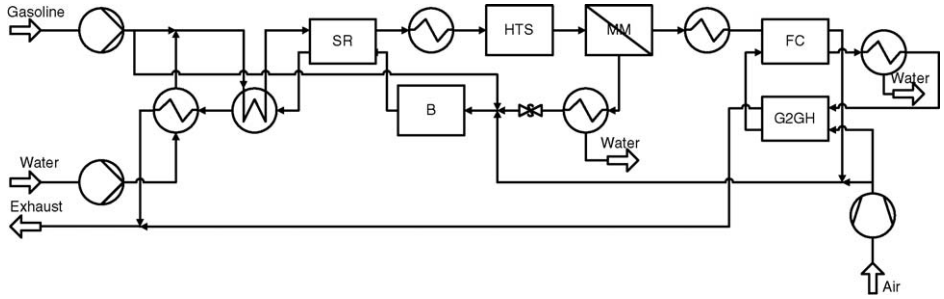

Fig. 1. Process flow diagram of system under examination.

hydrogen selective membrane (MM). Fig. 1 shows a flow sheet of the system.

Water is pumped to a heat exchanger, heated, evaporated and superheated to a temperature (400–600 °C) that is high enough to completely evaporate the gasoline injected afterwards. The educt mixture is preheated to the reformer's operation temperature (600–900 °C) and fed to its inlet. In the steam reformer, the following reactions take place simultaneously:

Steam reforming reaction:

$$-CH_2- + H_2O \Leftrightarrow CO + 2H_2, \quad \Delta H_R = 151\,\mathrm{kJ\,mol^{-1}} \tag{1}$$

Carbon dioxide-reforming:

$$CH_4 + CO_2 \Leftrightarrow 2CO + 2H_2, \quad \Delta H_R = 247\,\mathrm{kJ\,mol^{-1}} \tag{2}$$

Water–gas shift reaction:

$$CO + H_2O \Leftrightarrow CO_2 + H_2, \quad \Delta H_R = -41\,\mathrm{kJ\,mol^{-1}} \tag{3}$$

Methanisation:

$$CO + 3H_2 \Leftrightarrow CH_4 + H_2O, \quad \Delta H_R = -206\,\mathrm{kJ\,mol^{-1}} \tag{4}$$

Boudouard reaction:

$$2CO \Leftrightarrow C + CO_2, \quad \Delta H_R = -172\,\mathrm{kJ\,mol^{-1}} \tag{5}$$

Leaving the reformer, the reformate is cooled down to the inlet temperature of the high temperature shift (HTS) reactor (350–450 °C). The cooled reformate is supplied to the reactor where the water–gas shift reaction (Eq. (3)) takes place adiabatically. The product gas is subsequently fed to the membrane separation module. Almost pure hydrogen permeates through the membranes whereas the rest (steam, carbon monoxide, carbon dioxide and methane) leaves the module in the retentate.

The permeate is cooled down, fed to the PEMFC and converted almost completely. Unreacted hydrogen is led back to the inlet (not shown in the figure). From time to time the off gas is purged to the burner.

The air entering the fuel cell is compressed and humidified. The off gas of the cathode is cooled down, partly condensed and is used to humidify the air entering the fuel cell in the gas to gas humidifier (G2GH).

The retentate leaving the membrane is cooled down, the steam content is partly condensed and fed to the burner (B). Additional gasoline can be added to the burner's feed to supply sufficient heat to the reformer and the following heat exchangers.

The water that is condensed is pumped to a tank and recycled to the inlet (not shown in the figure).

3. Fuel processing and fuel cell system assessment criteria

There are numerous criteria to assess the potential of a fuel processing and fuel cell system such as:

- efficiency,
- weight,
- volume,
- emissions,
- integrability to a car's cooling system,
- start up time,
- capability to handle different loads,
- cost,
- complexity,
- ....

System's efficiency, weight and volume determine the potential for fuel savings through APUs and are therefore considered technical key criteria. In addition, the integrability of the APU to a car and its cooling system has to be guaranteed. Considering further criteria such as cost, start up time and emissions is beyond the scope of this work. The considered issues are explained in more detail in the following paragraphs.

3.1. System's efficiency

The efficiency of the overall system is described by the system's efficiency factor η_{Sys}. This efficiency factor relates the electrical power of the system $P_{el.,Sys}$ to the total energy supplied to the system in terms of the gasoline mole flow $\dot{n}_G$ fed to the reformer and burner and the corresponding lower heating value $h_{U,G}$:

$$\eta_{Sys} = \frac{P_{el.,Sys}}{\dot{n}_G \cdot h_{U,G}} \tag{6}$$

In terms of the efficiency of the subsystems the system's efficiency factor is given as:

$$\eta_{Sys} = \eta_{FPS} \cdot X_{FC} \cdot \eta_{FC} \cdot \eta_{Para} \tag{7}$$

where X_{FC} is the fractional conversion of the fuel cell, η_{FPS} and η_{FC} the efficiency factors of the fuel processing system and the fuel cell, respectively, and η_{Para} denotes the parasitic efficiency factor.

The efficiency factor of the actual fuel processing system η_{FPS} can be calculated as:

$$\eta_{FPS} = \frac{\dot{n}_{H_2,FC,in} \cdot h_{U,H_2}}{\dot{n}_G \cdot h_{U,G}} \tag{8}$$

It relates the energetic value of the hydrogen fed to the fuel cell $\dot{n}_{H_2,FC,in}$ (in this case, hydrogen permeated through the membrane) to the energetic value of the gasoline fed to the reformer and burner. This factor can be further distinguished into the efficiency factor of the reformer including the shift reactor and the efficiency factor of the membrane separation:

$$\eta_{FPS} = \eta_{Ref} \cdot \eta_{MM} \tag{9}$$

with

$$\eta_{Ref} = \frac{\dot{n}_{H_2,MM,in} \cdot h_{U,H_2}}{\dot{n}_G \cdot h_{U,G}} \tag{10}$$

and

$$\eta_{MM} = \frac{\dot{n}_{H_2,FC,in}}{\dot{n}_{H_2,MM,in}} \tag{11}$$

where $\dot{n}_{H_2,MM,in}$ is the mole flow of hydrogen supplied to the membrane separation module. The efficiency factor of the fuel cell can be written as the ratio of the electric power $P_{el.}$ to the energetic value of the hydrogen converted in the fuel cell or the ratio of actual (U_{FC}) to theoretical maximum voltage ($U_{theo.}$) of the fuel cell:

$$\eta_{FC} = \frac{P_{el.}}{X_{FC} \cdot \dot{n}_{H_2,FC,in} \cdot h_{U,H_2}} = \frac{U_{FC}}{U_{theo.}} \tag{12}$$

The parasitic efficiency factor is the ratio of usable electric power to the electrical power that is obtained from the fuel cell, given as:

$$\eta_{Para} = \frac{P_{el.,Sys}}{P_{el.}} \tag{13}$$

where $P_{el.,Sys}$ can be calculated as:

$$P_{el.,Sys} = P_{el.} - P_{Para}. \tag{14}$$

Accordingly, efficient systems are well configured and consist of:

- fuel cells requiring low hydrogen stoichiometries;
- fuel cells operating at high voltages;
- efficiently heated reformers with high hydrogen yield;
- hydrogen selective membranes;
- efficient pumps, compressors, etc. . . ..

3.2. Mass and volume of the system

As mentioned above, volume and mass of a fuel processing and fuel cell system are the key criteria. The exact determination of a system's volume requires a packaging for each system configuration, which is beyond the scope of this work. To compare the volumes of the different system configurations the volume of all components is summed up assuming that there are no system specific needs in the packaging later on. The considered volume is given as:

$$V_\Sigma = \sum V_i \tag{15}$$

where V_i denotes the volume of a single component.

The mass is obtained as follows:

$$m_\Sigma = \sum m_i \tag{16}$$

where m_i is the weight of a single component.

3.3. Integrability to the car's cooling system

The integrability of the APU to a car and its cooling system is necessary for its application. Thus, the minimum temperature in the system is determined by the car's cooling system. The minimum temperature is essential to the closure of the water balance. The closure of the water balance is necessary since no other fuel than the original fuel (gasoline) of the car is acceptable for the sake of customer's convenience. Therefore, the water has to be recycled and is obtained by partly condensing the retentate and cathode's off gas. Hence, the minimum condensation temperature allowing the closure of the water balance indicates the integrability to the car's cooling system.

4. Model

In order to evaluate the potential of the systems under examination the steady-state operation of the systems is modelled and simulated. The model of the overall system is comprised of the physical and chemical models of the system's components. These models and the underlying assumptions are explained in the following paragraphs. The modelling and simulation is conducted using Aspen Plus using both predefined modules and user-specified subroutines.

Model of gasoline: Gasoline is mixture of several hundred substances. Its composition depends on the manufacturer as well as on the charge. Hence, a model of gasoline is needed to conduct the above-mentioned modelling and simulations. Sommer [9] identified a mixture composed of *n*-heptane, *p*-xylene and cyclohexane of molar fraction 0.278, 0.396 and 0.326, respectively, to represent the total formula as well as the heating value with sufficient accuracy.

Equation of state: In the system under examination mainly gas phase reactions occur. Moreover, the gas is hydrogen rich. For this class of processes Aspen recommends the use of the Peng–Robinson equation [5]. The thermo-dynamic and transport properties of the liquid water are taken from steam tables.

Steam reformer: The steam reformer is modelled by using the predefined reactor type RGIBBS. It models phase and chemical equilibria simultaneously by minimising Gibbs free enthalpy considering all components that are specified [4]. In

the actual case, hydrogen, methane, carbon monoxide, carbon dioxide, water, carbon, nitrogen, oxygen, *n*-heptane, *p*-xylene and cyclohexane are specified.

Shift reactor: The predefined reactor REQUIL is used to model the high temperature shift reactor. By using this reactor the chemical equilibrium for the water–gas shift reaction is calculated (3).

Membrane separation: According to Lewis [7] the volumetric flow of hydrogen permeating through a palladium membrane can be written as:

$$\dot{V}_{H_2} = \frac{Q \cdot A}{d} \cdot (p^n_{1,H_2} - p^n_{2,H_2}) \tag{17}$$

where Q, A and d are the permeability, the surface and the thickness of the membrane, respectively. p_{1,H_2} and p_{2,H_2} denote the partial pressures of hydrogen on the corresponding sides of the membrane whereas n is constant depending on the load of the membrane. For little loads, n equals 0.5. In this case, the equation is known as Sievert's law.

The membrane is divided into several sections. For each section, the volumetric flow is calculated considering the decrease in the partial pressure of hydrogen with the run length.

PEM fuel cell: Due to the fact that pure hydrogen is fed to the stack, conversion in the fuel cell is assumed to be almost complete ($X_{FC} \simeq 1$). Accroding to Eq. (12), the efficiency factor of the fuel cell can be written as:

$$\eta_{FC} = \frac{P_{el.}}{X_{FC} \cdot \dot{n}_{H_2} \cdot h_{U,H_2}} = \frac{U_{FC}}{U_{theo.}} \tag{18}$$

In this work, a voltage U_{FC} of 720 mV is used.

Gas to gas humidifier: The gas to gas humidifier is modelled by a short-cut model. Due to this model steam is transferred through the membrane till a certain ratio of wet and dry gas partial pressures of steam is reached (Fig. 2).

Burner: The predefined reactor RGIBBS is used to model the burner. The stoichiometric ratio is adjusted to keep the adiabatic flame temperature in an acceptable range. An additional predefined heat exchanger (HEATER) is used to cool the burner's exhaust accounting for a heat loss.

Heat exchangers: Heat exchangers are assumed to be countercurrent exchangers and are modelled using the predefined module HEATX. The inlet and outlet temperature are set in a way to guarantee a minimum driving temperature difference ΔT_{min} of at least 25 K.

Jet pump: The jet pump is used to compensate for the pressure drop of recirculated gas in the following. A model of this jet pump has not been implemented jet. Therefore, the burden of the jet pump is quantified using two characteristic ratios—the entrainment and compression ratio. The entrainment ratio is given as:

$$ER = \frac{\dot{m}_s}{\dot{m}_m} \tag{19}$$

where $\dot{m}_s$ and $\dot{m}_m$ are the flow rates of the suction and motive gas, respectively. The compression ratio can be calculated as:

$$CR = \frac{p_{out}}{p_s} \tag{20}$$

where p_{out} and p_s denote the outlet and suction pressure, respectively.

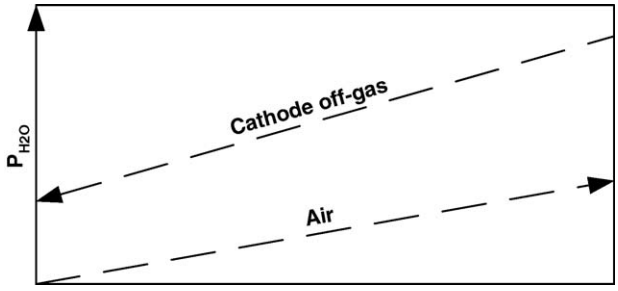

Fig. 2. Sketch of the gas to gas humidifier.

5. The concept of recirculating reformate

5.1. Motivation to recirculate reformate

Examining the influence of the operational parameters of the system under examination, the ratio of steam to carbon (S/C) fed to the reformer turns out to be of essential meaning:

- High S/C-ratios lead to significantly higher hydrogen yields increasing the reformer's efficiency factor η_{Ref}.
- High S/C-ratios result in lower hydrogen concentrations in the reformate decreasing the efficiency factor of the membrane separation η_{MM}.
- The steam fed to the reformer has to be heated, evaporated and superheated. Therefore, high S/C-ratios result in higher energy demands decreasing the fuel processing system's efficiency factor η_{FPS}.
- For mobile systems, the complete recovery of water is necessary. Hence, the excess water in the reformate has to be condensed. Due to the low boiling point the heat of condensation cannot be used by thermal intergration. Accordingly, the heat has to be removed through the cooling system. Therefore, high S/C-ratios result in higher energy demands and a lower parasitic efficiency factor η_{Para}.
- Low S/C-ratios are one of the reasons for catalyst deactivation.

Due to these facts there is a conflict in choosing a proper S/C-ratio.

Reviewing the system (Fig. 1), several steam-rich streams are identified. To partly recirculate these streams is proposed as a means to solve the above-described conflict by using the steam once evaporated and superheated in a more efficient way. The method is proposed in an analogy to Himmen and Strobel [3] who first proposed the recirculation of reformate to auto thermal reformers in corresponding fuel cell systems.

5.2. System configurations based on the recirculation of reformate

Looking for steam-rich streams in the process flow diagram of the actual system the following options for partly recirculating product gases are identified (see Fig. 3):

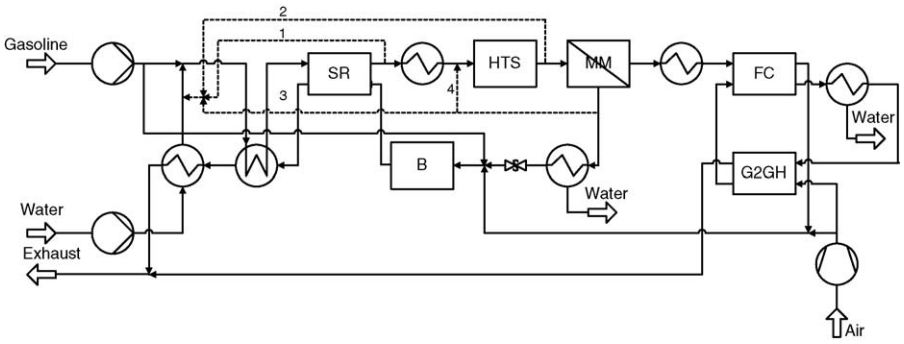

Fig. 3. Process flow diagram showing different options for partly recirculating product gases.

(1) recirculation of SR's off gases;
(2) recirculation of HTS's off gases;
(3) recirculation of MM's off gases;
(4) recirculating of MM's off gases to the HTS's inlet.

By recirculating product gases back to the educt stream following option (1–3) the educt gas composition of the SR is changed. Besides steam and gasoline, carbon dioxide, carbon monoxide, hydrogen, methane and recirculated steam are present. Hence, the steam to carbon ratio primary (0) given as

$$\left(\frac{\mathrm{S}}{\mathrm{C}}\right)_0 - \frac{\dot{n}_{\mathrm{H_2O}}}{\dot{n}_{\mathrm{C}}} = \frac{\dot{n}_{\mathrm{H_2O}}}{x \cdot \dot{n}_{\mathrm{C}_x\mathrm{H}_y}} \tag{21}$$

can be rewritten as

$$\left(\frac{\mathrm{S}}{\mathrm{C}}\right)_{\mathrm{R}} = \frac{\dot{n}_{\mathrm{H_2O}}}{\dot{n}_{\mathrm{C}}} = \frac{n_{\mathrm{H_2O,0}} + n_{\mathrm{H_2O,R}}}{x \cdot \dot{n}_{\mathrm{C}_x\mathrm{H}_y} + \dot{n}_{\mathrm{CH_4}} + \dot{n}_{\mathrm{CO}} + \dot{n}_{\mathrm{CO_2}}} \tag{22}$$

for the case of recirculated gases (R). Rewriting S/C this way, the amount of steam is not only related to the carbon content of hydrocarbons to be reformed. Thus, its character of a measure of catalyst-load changes. Therefore, a steam to hydrocarbon ratio (S/HC) is introduced in an analogy to $(S/C)_0$:

$$\frac{\mathrm{S}}{\mathrm{HC}} = \frac{\dot{n}_{\mathrm{H_2O,0}} + \dot{n}_{\mathrm{H_2O,R}}}{x \cdot \dot{n}_{\mathrm{C}_x\mathrm{H}_y} + \dot{n}_{\mathrm{CH_4}}} \tag{23}$$

If no reformate is recirculated, S/HC equals $(S/C)_0$. Through the recirculation of product gases, S/HC is changed. In the systems under examination, the mole flow of recirculated steam is always greater than the mole flow of recirculated methane. Hence, S/HC increases through the recirculation, if $(S/C)_0$ is kept constant. On the other hand, the recirculation allows to decrease $(S/C)_0$ if a constant S/HC is desired. Accordingly, two operational modes are distinguished:

(a) The recirculated gas is "simply" added to the educt stream before gasoline is injected ($(S/C)_0$ = const.). In this case, the S/HC is increased by the recirculation.
(b) The recirculated gas is added to the educt stream before the gasoline is added, but $(S/C)_0$ is decreased to keep S/HC constant.

Recirculating product gases following option (4), does not affect S/HC at the SR's inlet. Therefore, operational mode b does not apply in this case.

Table 1
Summary of system configurations and operational modes

Recirculation option	Operational mode a	Operational mode b
1	d-sr-a	d-sr-b
2	d-hts-a	d-hts-b
3	d-mm-a	d-mm-b
4	d-mm-hts-a	–

The following matrix shows a summary of possible system variations and introduces the nomenclature used in the following (Table 1).

6. Simulation results

In this section, simulations results are presented and discussed. For analysis purposes several variables are introduced in the first subsection. In Section 2, results of parameter studies are presented for each system. With respect to the introduced assessment criteria, results are given for a best efficiency and a fixed entrainment ratio parameter set. Based on these simulation results, the most interesting system is selected and discussed in detail in Section 3.

6.1. Variables for analysis purposes

In order to describe the recirculation of off gases quantitatively, the reflux ratio r is introduced as:

$$r = \frac{\dot{n}_{\mathrm{recirculated}}}{\dot{n}_{\mathrm{Splitter,in}}} \tag{24}$$

relating the mole flow of recirculated gas to the mole flow of gas supplied to the splitter. Moreover, the following dimensionless variables are defined to emphasise relative changes resulting from the recirculation. The system without recirculation ($r = 0$) is taken as reference (Table 2).

6.2. Simulation results

For each system parameter, studies have been conducted varying the reflux ratio r between 0 and 0.5 with a step size of 0.1. Reflux ratios greater than 0.5 result in less practicable entrainment ratios and partly require significant changes in the system configurations (e.g. the concept of thermal integration

Table 2
Variables for analysis purposes

Variable	Meaning	Definition
y_i^*	Normalised mole fraction	$y_i^* = \frac{y_i}{y_{i,0}}$
N_i^*	Normalised yield	$N_i^* = \frac{\frac{\dot{n}_{i,\mathrm{MM,in}}}{\dot{n}_{\mathrm{G,Ref,in}}}}{\frac{\dot{n}_{i,\mathrm{MM,in,0}}}{\dot{n}_{\mathrm{G,Ref,in}}}}$
η_j^*	Normalised efficiency factor	$\eta_j^* = \frac{\eta_j}{\eta_{j,0}}$
$T_{\mathrm{Cond.}}^*$	Normalised condensation temperature	$T_{\mathrm{Cond.}}^* = \frac{T_{\mathrm{Cond.}}}{T_{\mathrm{Cond.},0}}$
V^*	Normalised volume	$V^* = \frac{V_\Sigma}{V_{\Sigma,0}}$
m^*	Normalised weight	$m^* = \frac{m_\Sigma}{m_{\Sigma,0}}$

Table 3
Simulation results—best efficiencies

Variation-ID	r	η^*	$T_{\mathrm{Cond.}}^*$	V^*	m^*	ER	CR
d-sr-a	0.00	1.00	1.00	1.00	1.00	0.00	1.00
d-sr-b	0.30	1.02	0.98	1.04	1.07	0.43	1.01
d-hts-a	0.00	1.00	1.00	1.00	1.00	0.00	1.00
d-hts-b	0.30	1.01	0.98	1.06	1.09	0.43	1.02
d-mm-a	0.40	1.06	1.10	1.03	1.02	0.62	1.02
d-mm-b	0.40	1.07	1.10	1.00	0.98	0.62	1.02
d-mm-hts-a	0.50	1.02	0.97	1.06	1.01	0.95	1.01

has to be modified). Tables 3 and 4 show the simulation results for the parameter sets resulting in the best efficiencies (while stepwise varying r) and a certain entrainment ratios (ER = 0.5), respectively.

d-sr-a: The recirculation of the SR's off gases according to operational mode a (d-sr-a) has no positive impact on the system with respect to the introduced assessment criteria. Volume and weight increase through the recirculation while the system's efficiency and the condensation temperature remain unaffected (Table 4). Since the efficiency is not influenced, the recirculation ratio is chosen to be zero for the best efficiency set of results (Table 3).

Taking into consideration that the SR is modelled as reactor reaching equilibrium state, these results are understandable. A certain group of species is allowed to reach equilibrium state. Afterwards a non-selectively chosen part of these species is recirculated and fed to the educt stream. The mixture is allowed to reach equilibrium again. Since the composition of species did not change, the resulting equilibrium composition of product components is not influenced either.

Table 4
Simulation results—fixed entrainment ratio ER = 0.5

Variation-ID	r	η^*	$T_{\mathrm{Cond.}}^*$	V^*	m^*	ER	CR
d-sr-a	0.33	1.00	1.00	1.07	1.11	0.50	1.01
d-sr-b	0.33	1.02	0.98	1.06	1.09	0.50	1.01
d-hts-a	0.33	1.00	1.00	1.09	1.14	0.50	1.02
d-hts-b	0.33	1.01	0.98	1.07	1.11	0.50	1.02
d-mm-a	0.35	1.06	1.09	1.02	1.01	0.50	1.02
d-mm-b	0.35	1.08	1.09	1.00	0.98	0.50	1.02
d-mm-hts-a	0.35	1.02	0.97	1.03	1.00	0.50	1.01

d-sr-b: Recirculating the SR's off gases while keeping S/HC constant, allows to decrease $(S/C)_0$ (d-sr-b). It can be seen, that an increase of 2% in the overall system's efficiency follows from reflux ratios $r = 0.3$ and 0.33 (Tables 3 and 4). The enhancement in system's efficiency is going along with a decrease in condensation temperature (−2%) and increases in system's volume (+4%) and weight (+7%).

d-hts-a: In an analogy to d-sr-a, the recirculation of HTS' off gases according to operational mode a has no positive affect on the system.

d-hts-b: An increase in system efficiency (+1%) accompanied with a decrease in condensation temperature (−2%) and an increase in the volume (+6%) and weight (+9%) of the system can be observed similar to d-sr-b (Table 3).

d-mm-a: Recirculating the MM's off gases according to operational mode a, leads to enhancements of 6% in the system's efficiency and increases of 10% in the condensation temperature. These effects go along with increases in the volume and weight by 3 and 2%, respectively.

d-mm-b: The best efficiency parameter set was obtained from the stepwise variation of the reflux ratio (Table 3). To obtain an entrainment ratio ER = 0.5 the corresponding reflux ratio was found to be 0.35 (Table 4). This reflux ratio is obviously closer to the true maximum efficiency. The recirculation of MM's off gases keeping S/HC constant, results in increases of the system's efficiency of 8% and increases of the condensation temperature of 9%. The volume remains constant whereas the weight decreases by 2%.

d-mm-hts-a: The simulation of this case requires an additional assumption, since the motive gas of the jet pump is the SR's off gas. Accordingly, the pressure of the motive gas cannot be simply increased as in the other cases where steam is used as motive gas. In this case, the pressure drop over the jet pump is assumed to be 1 bar. Under this assumption, the recirculation of MM's off gases to the HTS's inlet results in increases of the system's efficiency of 2%, a decrease in the condensation temperature of 3% accompanied by an increase in volume of 3%. The weight is constant in this case.

6.2.1. Summary

The simulation results for the recirculation of MM's off gases are visualised in Fig. 4. The results show that the recirculation of MM's off gases lead to significant enhancements in system's efficiency and considerable increases of the condensation temperature. For d-mm-a, these benefits go along with moderate increases in system's volume and weight, whereas these changes are negligible for d-mm-b. Therefore, d-mm-b is considered to be the most interesting option and a detailed analysis of the system is given in the following subsection.

6.3. Simulation results for d-mm-b

In this section, the simulation results for the d-mm-b are presented and discussed in detail. In the first paragraph, the impact of recirculation on the system's efficiency is analyzed. The anal-

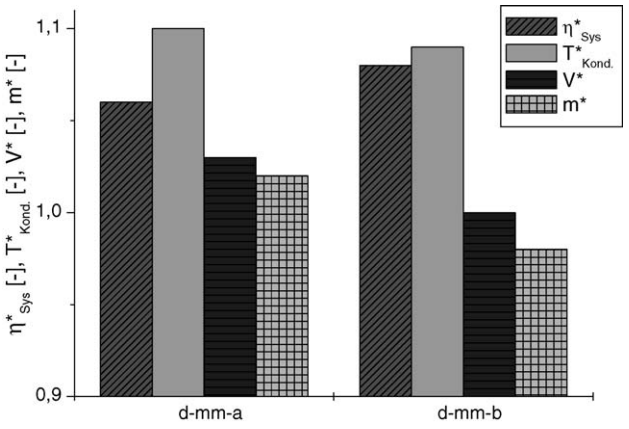

Fig. 4. Dimensionless assessment criteria for d-mm-a ($r = 0.4$) and d-mm-b ($r = 0.35$).

ysis includes the efficiencies of the subsystems, the hydrogen concentration and yield as well as the primary steam to carbon ratio $(S/C)_0$ and the steam to hydrocarbon ratio S/HC. In the second paragraph, the influence of the recirculation on the condensation temperature is examined. The effects on the system's volume and weight are explained in the third paragraph followed by short discussion on the jet pump's burden.

6.3.1. Impact on system's efficiency

The effects of the recirculation on system's and subsystem's efficiency factors are visualised in Fig. 5. The efficiency factor of the overall system η_{Sys} initially increases with the reflux ratio r and reaches a maximum at $r = 0.4$. The overall efficiency factor is a function of the fuel cell's (η_{FC}), the fuel processing system's (η_{FPS}) and the parasitic (η_{Para}) efficiency factor. While η_{FC} remains constant, η_{Para} and η_{FPS} increase.

η_{FPS} is the product of the efficiency factors of the reformer (η_{Ref}) and the membrane separation (η_{MM}). η_{Ref} relates the energetic value of the hydrogen reformed to the energetic value of gasoline that is burned and reformed. Therefore, one reason for an increase of this factor is an increase in the hydrogen mole flow

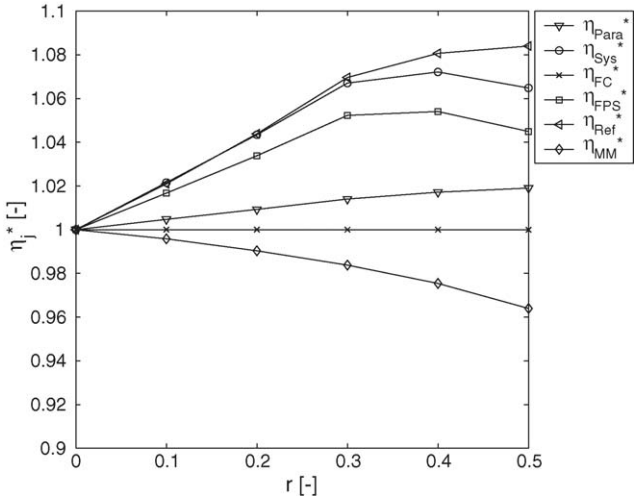

Fig. 5. Normalised efficiency factors η_j^* over the reflux ratio r.

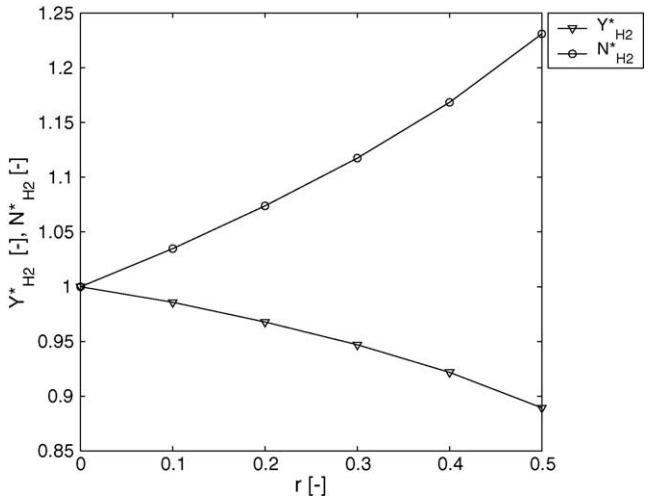

Fig. 6. Normalised hydrogen mole fraction $Y_{H_2}^*$ and yield $N_{H_2}^*$ over reflux ratio r.

and the hydrogen yield, respectively. The normalised hydrogen yield is plotted as a function of the reflux ratio in Fig. 6. Form the curves of η_{Ref} and $N_{H_2}^*$, one can conclude that recirculation becomes costly in terms of gasoline that is burned with increasing reflux ratios. The other factor influencing η_{FPS} is η_{MM}, which depends on the hydrogen concentration in the MM's feed. The dependency of the hydrogen concentration on the reflux ratio is plotted in Fig. 6 as well. The corresponding decrease in η_{MM} can be seen in Fig. 5. The graph of η_{FPS} results from the interplay of η_{Ref} and η_{MM}. η_{Para} is relating the electric power available to the user $P_{el.,Sys}$ to the total electric power of the fuel cell $P_{el.}$. The dominating sources of parasitic loss are the fan used in the cooling cycle for heat removal and the compressor supplying the air to the fuel cell and the burner. Both the electric power of the fan and the compressor depend partly on the primary steam to carbon ratio $(S/C)_0$. Fig. 7 shows the decrease in $(S/C)_0$ over the reflux ratio keeping S/HC constant leading to the increase in η_{Para} (Fig. 5).

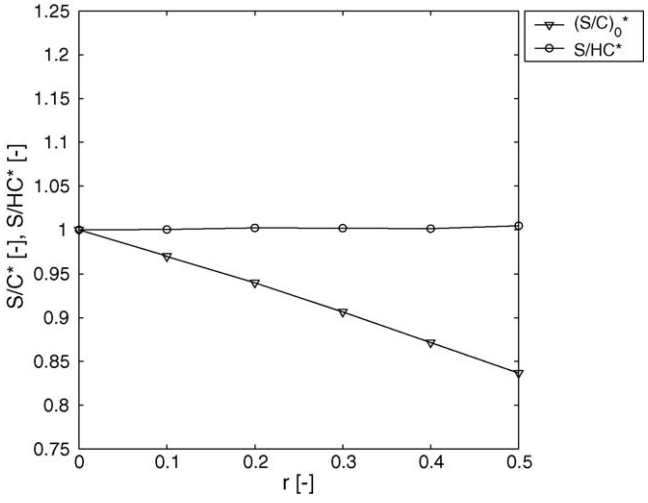

Fig. 7. Normalised primary steam to carbon ratio $(S/C)_0^*$ and normailzed steam to hydrocarbon ratio S/HC^* over reflux ratio r.

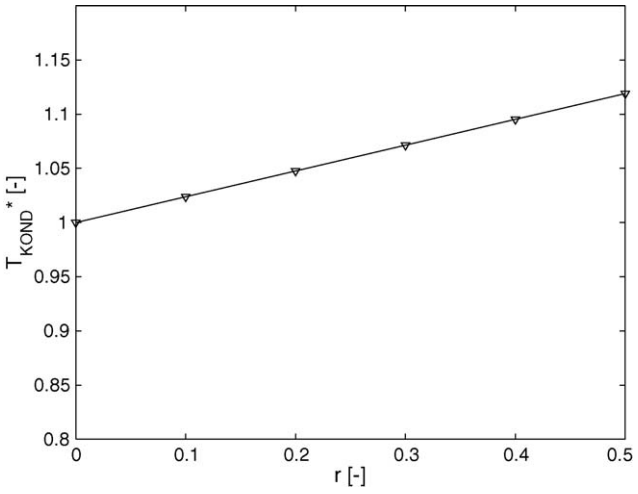

Fig. 8. Normalised condensation temperature $T^*_{\text{Cond.}}$ over reflux ratio r.

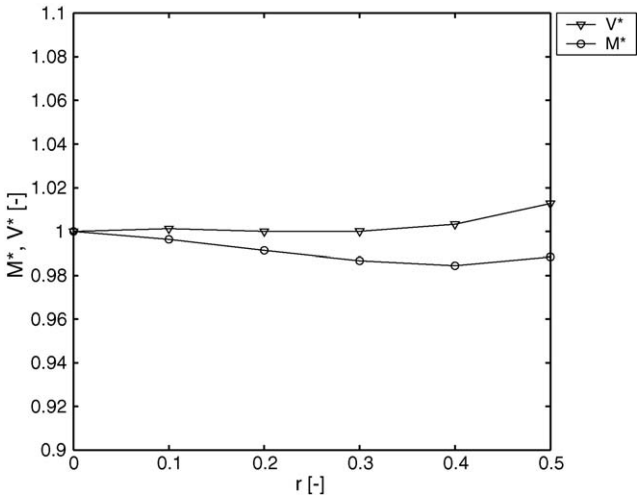

Fig. 11. Normalised volume V^* and weight m^* over reflux ratio r.

6.3.2. Impact on condensation temperature

The effect of recirculation on the condensation temperature is visualised in Fig. 8. To clarify this increase in condensation temperature, a main issue of closing the water balance is explained by the use of the atomic balance of hydrogen. As shown in Fig. 9, a certain mole flow of hydrogen is fed to the FPS and subsequently to the MM. The hydrogen is bound in hydrogen, steam and methane molecules. The hydrogen permeating through the membrane is fed to fuel cell and converted. A certain part of it can be obtained bound in water through condensation. Hence, the hydrogen permeating through the membranes contributes to the closure of the water balance.

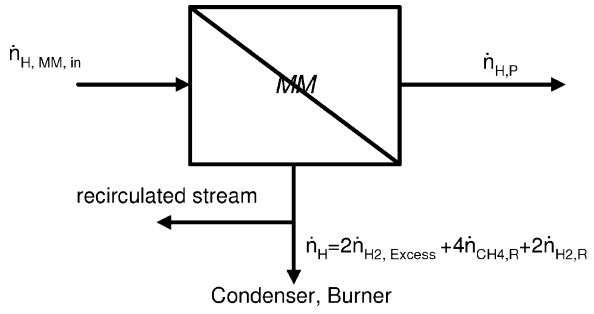

Fig. 9. Sketch of atomic balance.

From the hydrogen in the retentate supplied to the condenser and the burner only the hydrogen bound in the steam can contribute to the closure of the water balance whereas the hydrogen being part of hydrogen and methane molecules cannot.

Therefore, reducing the mole flows of hydrogen and methane fed to the burner is a means of increasing the condensation temperature. By partly recirculating the MM's off gases to the SR this can be done. For analysis purposes B is defined as the mole flow of hydrogen fed to the burner over the total flow of hydrogen fed to the fuel processing system:

$$B = \frac{\dot{n}_{\text{H,Burner,in}}}{\dot{n}_{\text{H,FPS,in}}} \tag{25}$$

Again, the case without recirculation is used as reference case in order to define B^*. The decrease in B^* (e.g. the reduction

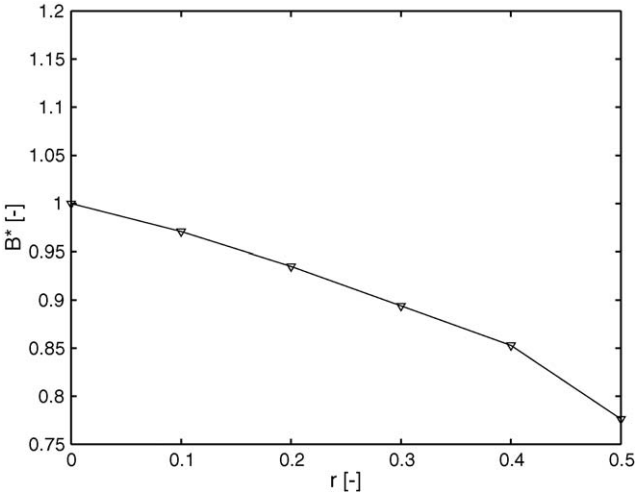

Fig. 10. Normalised portion of hydrogen supplied to the burner B^* over reflux ratio r.

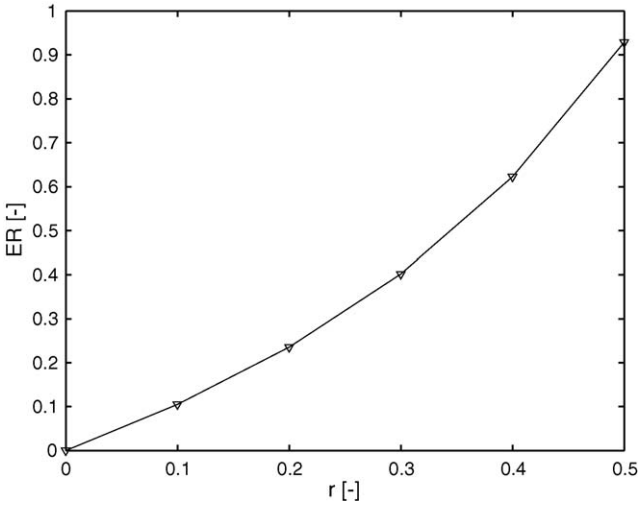

Fig. 12. Entrainment ratio ER over reflux ratio r.

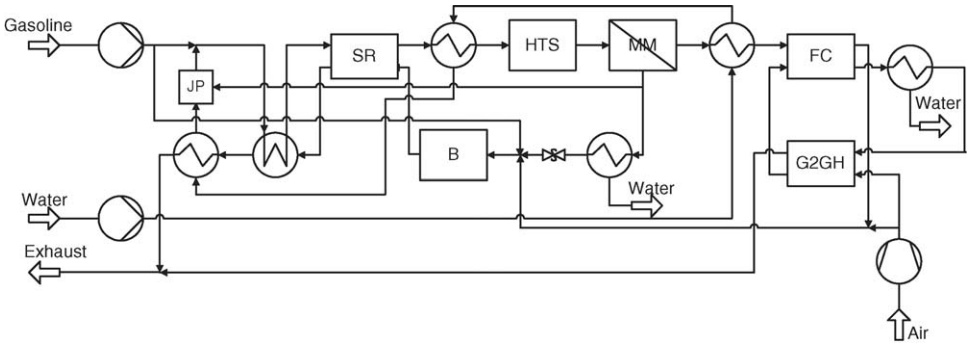

Fig. 13. Process flow diagram of d-mm-x.

of "lost/burned" hydrogen) with reflux ratio r can be seen in Fig. 10. Due to this explanation the similarity of the effect of recirculation on the condensation temperature for d-mm-a and d-mm-b is understandable.

6.3.3. Impact on volume and mass

Fig. 11 shows the effect of the recirculation on system's volume and weight. Keeping all feed streams to the fuel processing system constant, the recirculation of gases would increase the volume and weight of the system. However, the enhancement in overall system efficiency offers the possibility to reduce the size of the fuel processing system keeping the electric power of the fuel cell system constant. Both effects superpose leading to negligible changes in mass and volume as shown in the figure.

6.3.4. The jet pump's burden

The burden of a jet pump is usually described by the entrainment ratio ER, the compression ratio CR, and the ratio of suction to motive pressure [2]. In Fig. 12, the entrainment ratio for d-mm-b is plotted over the reflux ratio r. The compression (1.01–1.02) and entrainment (0.0–1.0) ratios for all cases under examination are small. Moreover, in the actual system steam is used as motive gas (Fig. 13). Therefore, the only restriction on the motive pressure is that water should be vaporised at the operation temperature of the jet pump, which is between 350 and 450 °C. According to this restriction, ratios of suction to motive pressure smaller than 0.1 are possible. Hence, it seems reasonable to expect the jet pump to be capable of these loads.

7. Summary and outlook

The recirculation of reformate is a means of efficiency enhancement in gasoline reforming. Several systems derived from this idea have been simulated and discussed with respect to the system's efficiency, volume, weight and the maximum condensation temperature. Significant improvements in the system's efficiency (up to 8%) as well as considerable increases in the condensation temperature (up to 10%) accompanied by small or negligible changes in volume and weight have been obtained for the recirculation of MM's off gases. Based on these results, future activities will focus on the experimental validation of the described phenomena. An additional positive effect of recirculation is expected concerning the functionality of the overall system. The presence of hydrogen and carbon dioxide while evaporating gasoline, superheating and reforming the educt mixture is expected to have a positive impact on the system's lifetime.

References

[1] M. Cassier, C. Bernay, M. Marchand, Prospects of different fuel cell technologies for vehicle applications, J. Power Sources 108 (June) (2002) 139–152.
[2] L.A. DeFrate, A.E. Hoerl, Optimum design of ejetors using digital computers, Chem. Eng. Prog. 55 (1959) 43–50.
[3] M. Himmen, B. Strobel, DE 19934649, 2001.
[4] Aspen Plus Inc., Reference Manual, vol. 1, Unit Operation Models, Release 9, 1996.
[5] Aspen Plus Inc., Reference Manual, vol. 2, Physical Property Methods and Models, Release 9, 1996.
[6] F. Fineschi, L. Petruzzi, S. Cocchi, A global thermo-electrochemical model for sofc system design and engineering, J. Power Sources 118 (May) (2003) 96–107.
[7] F.A. Lewis, The Palladium–Hydrogen System, Academic Press, New York, 1967.
[8] E. Carlson M. Straraonova, S. Lasher, Assessment of fuel cell auxiliary power systems for on-road transportation applications, Progress Report, FY, 2003.
[9] M. Sommer, Entwicklung eines Benzinreformers fur mobile Anwendungen, Ph.D. Thesis, Universitat Dortmund, 2003.
[10] D. zur Megede, M. Sommer, On-board hydrogen production for fuel cell applications in vehicles, DGMK-Conference, Dresden, October 2003, pp. 147–162.